Marine Chemistry 149 (2013) 74–84

Contents lists available at SciVerse ScienceDirect

Marine Chemistry

journal homepage: www.elsevier.com/locate/marchem

Porewater temporal variability in a wave-impacted permeable nearshore sediment

Kristen E. Fogaren *, Francis J. Sansone, Eric H. De Carlo

Department of Oceanography, University of Hawai'i at Mānoa, 1000 Pope Rd, Honolulu, HI 96822, USA

ARTICLE INFO

Article history:
Received 19 July 2012
Received in revised form 6 December 2012
Accepted 17 December 2012
Available online 5 January 2013

Keywords:
Permeable sediment
Sandy sediment
Surface gravity waves
Nutrient cycling
Oxygen
Remineralization rate
DIC

ABSTRACT

Porewater samples were collected from a nearshore permeable sediment on Oahu, Hawaii over a variety of surface gravity wave conditions to evaluate the effect of ocean swells and their corresponding bottom currents on porewater dissolved oxygen and inorganic nutrient dynamics. Our results indicate that swells with significant wave heights of ~1.3 m, with resulting nearbed velocities reaching at least 0.30 m s^{-1}, flush the porewater to a depth of ~7.5 cm by enhancing exchange between the upper sediment and the overlying water column. Upper-sediment dissolved oxygen inventories were positively correlated with nearbed velocities, and decline linearly versus time during background conditions following upper-sediment flushing, corresponding to an apparent upper-sediment deoxygenation rate of 0.31 mmol $m^{-2}d^{-1}$. Similarly, upper-sediment nutrient inventories were observed to recover linearly after swell events, resulting in sediment recovery rates for silicate and soluble reactive phosphate of 35 μmol $m^{-2}d^{-1}$ and 3.5 μmol $m^{-2}d^{-1}$, respectively. The observed elemental ratios of regenerated nutrients suggest that the majority of organic matter undergoing remineralization is planktonic in origin. Wave-enhanced exchange is associated with a fluorescence response in the bottom of the overlying water column, suggesting that sediment flushing and subsequent nutrient input to the water column may be important to nutrient budgets and photosynthetic communities in nearshore oligotrophic waters.

1. Introduction

Although sandy, highly permeable sediments cover ~44% of the world's continental shelves (Riedl et al., 1972), the role of these sediments in coastal biogeochemical cycles has historically, for several reasons, been neglected (Boudreau et al., 2001). Notably, conventional methods for sampling fine-grained sediments (e.g., coring, benthic chambers) either do not work or disrupt the sandy sediment structure (Boudreau et al., 2001; Jahnke, 2004). Also, permeable sediments typically have a lower organic matter content compared to their fine-grained counterparts (Boudreau et al., 2001; Meyer-Reil, 1986), resulting in the misperception that permeable sediments have relatively low biogeochemical activity (Boudreau et al., 2001; Rocha, 2008).

However, high oxygen consumption rates coupled with low organic matter content in permeable sediments suggest that these sediments may be sites of high biogeochemical activity and efficient organic matter remineralization (Huettel et al., 1998; Rocha, 2008; Webb and Theodor, 1968), even matching metabolic rates found in organic-rich, fine-grained sediments (Jahnke et al., 2000, 2005).

Permeable sediments can support high metabolic rates through several mechanisms of enhanced fluid and particle transport between the water column and porewater. First, enhanced porewater flow can result from pressure gradients created by bottom currents flowing over small topographic features such as sediment ripples, infauna mounds and benthic fauna (Boudreau et al., 2001; Huettel and Gust, 1992; Huettel et al., 1996). Second, surface gravity waves are important drivers of enhanced transport in permeable sediments in wave-impacted environments (e.g., Falter and Sansone, 2000a); as surface gravity waves pass over a permeable sediment, they cause a dynamic pressure field that can induce porewater movement and thereby control chemical zonation in carbonate sands (Boudreau et al., 2001). Last, enhanced porewater flow can force degradable particles like bacteria, algae, diatoms and detritus into the sediment where they can be retained (Huettel and Rusch, 2000; Huettel et al., 1996), thereby increasing the transfer rate of particulate matter across the sediment-water interface. Furthermore, enhanced porewater flow can result in particles penetrating deeper into the sediment than what typically occurs through simple gravitational settling (Huettel et al., 1996). For example, Rusch and Huettel (2000) demonstrated that bottom currents can physically force diatoms ~2.2 cm into a permeable sediment. Oxygen and other electron acceptors that are flushed through the sediments, enhance particle decay, resulting in the high metabolic rates found in permeable sediments (Boudreau et al., 2001).

Remineralized constituents are also transferred to the overlying water column at enhanced rates (Huettel et al., 1998). In oligotrophic waters, inorganic nutrients produced by remineralization within the sediments may be an important source of nutrients to the water

* Corresponding author. Tel.: +1 808 9568370.
E-mail addresses: fogaren@hawaii.edu (K.E. Fogaren), sansone@soest.hawaii.edu (F.J. Sansone).

0304-4203/$ – see front matter © 2013 Elsevier B.V. All rights reserved.
http://dx.doi.org/10.1016/j.marchem.2012.12.005

column. For example, in a year-long study of coral reefs on the southern shore of O'ahu, Hawai'i, water-column concentrations of dissolved nitrate and ammonium were seen to increase during three ocean swell events (Grigg, 1995). Therefore, the connection between sediment organic matter remineralization, inorganic nutrient production, and water-column productivity may be important in coastal systems with permeable sediments, and may be regulated by physical forcing.

We report here on porewater inorganic nutrient and dissolved oxygen dynamics in a well-monitored permeable nearshore sediment environment. Samples were collected under a variety of surface gravity wave conditions in order to evaluate the effect of ocean swells and their corresponding bottom currents on porewater dissolved oxygen and nutrient dynamics. Our results suggest that swell-induced flushing of the sediment affects porewater dissolved oxygen and inorganic nutrients concentrations to a depth of ~7.5 cm, and that this process is associated with an apparent photosynthetic response in the bottom water.

2. Study area

Our 12-m deep study site was located at the Kilo Nalu Nearshore Reef Observatory in Māmala Bay on the south shore of O'ahu, Hawai'i (Fig. 1; Sansone et al., 2008). The existing infrastructure at Kilo Nalu allowed in situ physical data to be accessed in near real-time.

2.1. Swell conditions

The south shore of O'ahu can be characterized as having four types of ocean swells (Fletcher et al., 2002). The first and most common is the Trade Wind Swell originating from the northeast (~45°) and wrapping around the southern flank of Diamond Head (Fig. 1). These swells persist most of the year and have typical wave heights of 0.3 to 1.3 m, with periods of 5–8 s (Fletcher et al., 2002). The second type is the Southern Swell that is generated in the southern hemisphere by austral winter storms. These occur mostly in summer and early autumn, from April to October; they are usually from the south (~180°) but can originate anywhere from 147° to 210° (Fletcher et al., 2002). The Southern Swell typically results in waves ranging from 0.3 to 1.2 m in height with 14- to 22-s periods, but can result in waves as high as 5.5 m with 25-s periods in fully developed seas (Fletcher et al., 2002; Moberly and Chamberlain, 1964). The third type of swell is associated with what are locally known as Kona Storms. These storms are generated by local atmospheric low pressure systems, with ocean waves developing from southerly to southwesterly winds (Moberly and Chamberlain, 1964). These storms can occur at any time of the year, but are more common in winter, and result in 0.9- to 1.5-m waves with 8- to10-s periods (Fletcher et al., 2002), although waves reaching heights of 5 m have been observed under extreme circumstances (Moberly and Chamberlain, 1964). The fourth and least frequent type of swell that impacts the south shore is a hurricane-related swell (Fletcher et al., 2002).

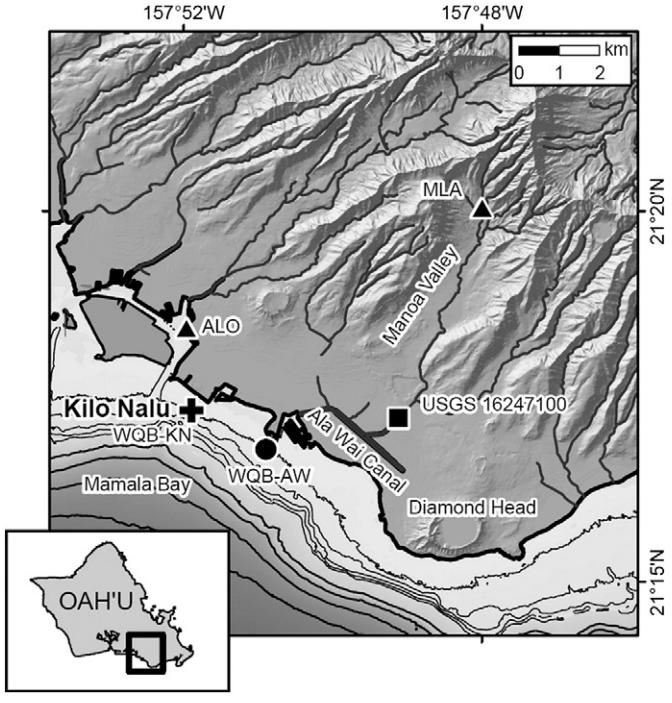

Fig. 1. Map of Māmala Bay and southern O'ahu, including the Ala Wai watershed. Kilo Nalu Observatory is indicated with a black cross. The two rain gauge sites, Mānoa Lyon Arboretum (MLA) and Aloha Tower (ALO), are indicated with black triangles, and USGS stream discharge gauge 16247100 is indicated with a black square. Water quality buoys are located south of the Ala Wai Canal (WQB-AW, black circle) and at Kilo Nalu Observatory (WQB-KN, black cross). Depth contours are shown every 10 m (thin black lines) and every 100 m (thick black lines) until 400 m.

2.2. Ala Wai Watershed

The Ala Wai Canal is a channel that drains the Ala Wai Watershed and is one of three main freshwater sources for Māmala Bay (Fig. 1; Fryer, 1995; Laws et al., 1999). A United States Geological Survey (USGS) stream gauge located on the Mānoa-Pālolo Drainage Canal (USGS 16247100), a few hundred meters inland of the Ala Wai Canal, provides stream flow rates. National Weather Service (NWS) rain gauges collect rainfall data at 15-min intervals at the Mānoa-Lyon Arboretum (MLA) in Mānoa Valley and in downtown Honolulu at Aloha Towers (ALO).

3. Methods

3.1. Measurement of wave and water-column characteristics

The instruments utilized in this study were deployed at the Kilo Nalu Nearshore Observatory in 12 m of water, approximately 400 m from shore (Fig. 1). They included a 1200-kHz acoustic Doppler current profiler (ADCP) (RDI-Teledyne, Poway, CA, USA), a Seabird-37 conductivity-temperature-depth (CTD) recorder (Sea-Bird Electronics, Inc., Bellevue, WA, USA) and an ECO FLNTU sensor (WET Labs, Philomath, OR, USA). The ADCP measured near-bed current velocity, surface wave characteristics, and tide levels. The CTD measured conductivity, temperature and pressure, enabling physical water properties (salinity, density and depth) to be determined. The ECO FLNTU sensor measured turbidity and fluorescence ~0.5 m above the sediment-water interface (SWI) as proxies of particle matter loading and biological primary productivity, respectively (Sansone et al., 2008).

The bottom-mounted, upward-looking ADCP was deployed continuously and was configured to collect high-resolution ensemble pressure and velocity data at 1 Hz. Velocity readings were collected starting at 0.45 m above the SWI, continuing upward throughout the water column at a vertical resolution of 25 cm, with an accuracy of ± 0.003 m/s and resolution of ± 0.001 m/s. Current velocities were averaged every 20 min, and wave data presented in this study were calculated over 20-min periods, the shortest period of time over which wave statistics could be reasonably calculated. Significant wave height (H_{sig}) was determined by the spectral method (Emery and Thomson, 2004), in which H_{sig} is equal to 4 times the integral of the power spectrum (wave energy as a function of frequency); this is equivalent to the mean height of the one-third largest waves.

Nearbed velocity (V_{bed}) was used as a measure of wave-induced velocity and wave period, and was defined as the mean of the highest one-third of the velocity readings recorded in the bottom 3 m of the water column. V_{bed} is correlated with H_{sig} ($V_{bed} = 0.19H_{sig} + 0.054$;

$R^2 = 0.61$; $n = 72125$) and is used here to quantify physical conditions close to the SWI.

Additionally, two surface water quality buoys (WQBs) were equipped with Seabird-16*plus* V2 SEACAT C-T recorders and ECO FLNTU sensors to provide conductivity, temperature, fluorescence and turbidity measurements ~0.5 m below the surface. As a part of the Pacific Island Ocean Observing System (PacIOOS) described by Tomlinson et al. (2011), the first buoy was located 335 m from the mouth of the Ala Wai Canal (WQB-AW) and the second was located at Kilo Nalu Observatory (WQB-KN), situated ~2 km west of the Ala Wai Canal mouth (Fig. 1).

3.2. Sampling and analysis of sediment

The sediment at Kilo Nalu consists of coral, limestone and other carbonate material (Sansone et al., 2008). A grab sediment sample was manually collected by divers to characterize the top ~10 cm of sediment near the porewater wells (described in Section 3.3). X-ray diffraction (XRD) analysis was performed on ground sediment to determine mineralogical content. An estimate of the sediment organic content was determined in triplicate by loss-on-ignition (LOI). This method works well in carbonate sediments with low clay content (Dean, 1974), such as those found at Kilo Nalu. The common interferences of the LOI method, such as dehydration of clay minerals or metal oxides, loss of volatile salts, or loss of inorganic carbon in minerals (e.g., siderite, magnesite or rhodochrosite; Heiri et al., 2001), are likely low in our sediments. Grain size analysis was performed in triplicate on the post-combusted sediment.

3.3. Sampling and analysis of porewater

Six porewater sampling wells, each 1 m in length, were constructed using 1.25-cm outer diameter, 0.75-cm inner diameter PVC pipe and PVC ball valves (Falter and Sansone, 2000a, 2000b). Each well had a sampling port at a specified depth. Porewater wells with collection depths at 7.5, 15, 20, 30, 40 and 50 cm below the SWI were manually installed by divers in the sand patch at the Kilo Nalu 12-m site. A more detailed description of porewater well installation is given by Fogaren (2010). The wells were deployed in a rectangular 20×10 cm area, and the arrangement of the wells ensured close proximity of adjacent wells, while minimizing interference between wells (Falter and Sansone, 2000b). Assuming a porosity of 0.49 (Hebert et al., 2007) and a spherical porewater sample volume of 140 mL, the sphere of sediment which was sampled was ~4 cm in radius. It should be noted that, although this type of porewater well is commonly used, the effect on boundary layer hydrodynamics has not been quantified.

Discrete porewater samples were collected on 29 separate occasions over a variety of physical conditions over a 29-month period beginning on 26 August 2007 and ending on 29 January 2010. Time spans between sampling dates varied from 2 days to 6 months. Intensive sampling was carried out during June–December 2008, with 18 samplings within that 6-month period. During a large swell event in late summer 2008, the wells were partially scoured out of the sediment and were no longer at their intended depths. As a result, the original porewater array, which was installed in early 2006, was removed and replaced with a new array on 7 October 2008.

A porewater sample from each well, as well as a seawater sample from the SWI, was collected manually by divers on each sampling date using 140-mL Monoject plastic syringes (Covidien, Mansfield, MA, USA), for a total of 7 samples for each sampling day. The SWI sample was collected 2–3 mm above the SWI using Tygon tubing connected by a three-way stopcock to a syringe. Porewater sample collection from each well began after the dead volume in the well was removed in order to guarantee sampling from the desired sediment depth. The dead volume was removed by drawing and discarding a predetermined volume of water, which varied depending on the collection depth. Once collected in the syringes, porewater samples were taken to the surface for subsampling.

Dissolved oxygen (DO) was measured in the field using a Thermo Scientific Orion 3 Star Portable dissolved oxygen meter with a Clark-type electrode (Thermo Electron Corp., Beverly, MA, USA) while the subsample was stirred continuously in a 20-mL Wheaton (Wheaton Industries Inc, Millville, NJ, USA) glass serum vial. The electrode was calibrated in the field using a Thermo Scientific air calibration sleeve immediately before processing samples. The relative accuracy of DO measurements was 6 μM, with a limit of detection of 0.6–1.6 μM. The instrument's zero offset was later removed from the DO measurements (see Data Corrections below).

The remaining porewater was filtered manually through precombusted Whatman GF/F filters (25-mm diameter, nominal pore size of 0.7 μm; GE Healthcare, UK) held in plastic Whatman Swin-Lok filter holders (GE Healthcare, UK). All subsamples for dissolved inorganic nutrients were frozen and later analyzed in duplicate for soluble reactive phosphate (SRP) and silicate ($Si(OH)_4$). Both SRP (± 0.06 μM) and $Si(OH)_4$ (± 0.24 μM) were determined using standard colorimetric methods (Grasshoff et al., 1983) with a BioTek Synergy HT Multi-Mode Microplate Reader (BioTeck, Winooski, VT, USA) using Nunc 96 well optical-bottom plates (Nalge Nunc International, Rochester, NY, USA) with a 1-cm pathlength. Analytical triplicates were used when unreasonable differences were encountered between duplicates, and a Q-test was then used to determine whether to remove replicates (Skoog et al., 1994). The limits of detection for SRP and $Si(OH)_4$, were 0.26 μM and 0.48 μM, respectively.

Dissolved inorganic carbon (DIC) subsamples were filtered as previously described and preserved in 20-mL glass serum bottles using 50 μL of a saturated aqueous mercuric chloride solution (Dickson et al., 2007). Samples for DIC (± 0.02 mM) were collected only on 25 November 2008, 2 December 2009, 18 December 2009 and 29 January 2010. DIC samples were analyzed in duplicate, with a limit of detection of 0.02 mM, using a Model 5011 CO2 Coulometer (UIC, Inc; Joliet, IL, USA).

Mohr chlorinity titrations (Grasshoff et al., 1983) were performed to determine salinity, with a relative precision of 0.4%, using IAPSO Standard Seawater (OSIL, Havant, Hampshire, UK) as a reference material.

3.4. Data corrections

Sediment height at the porewater wells varied (± 3 cm) because of scouring or burial of the wells in the active environment at Kilo Nalu. Divers recorded the actual sampling depths of each well while sampling. Results reported here give the actual depth below the SWI, not the intended sampling depth.

Two types of corrections were applied to the porewater DO data. The first was an instrumental zero correction. Instrumental zero was calculated by measuring DO in seawater that had been sparged with nitrogen for 30 min to remove the oxygen, and was determined be 0.06 μM. The second correction compensated for oxygen contamination of the porewater samples. This contamination resulted from oxygen-depleted porewater being held in semi-gas-permeable plastic sampling syringes that were exposed to oxygen-saturated seawater and the atmosphere before analysis. A laboratory experiment that simulated field conditions determined that contamination increased logarithmically over time: $y = 6.9343\ln(t) + 2.428$ ($R^2 = 0.9732$), where t is time (min) elapsed since sampling and y is the DO contamination (μM). Syringes were exposed for an average of 20 min, with a maximum exposure time of 40 min, before samples were analyzed for DO, resulting in an average DO contamination correction of ~23 μM, with a maximum DO contamination correction of ~28 μM. When exact sampling times for individual sampling syringes were not available, average t values from other samplings were used due to the systematic nature of sampling. More detailed descriptions of these corrections are given by Fogaren (2010).

Instrument biofouling is often a concern in tropical waters with a large amount of light penetration. Although equipped with its own rubber wiper and copper faceplate to deter biofouling, significant biological growth occurred on the ECO FLNTU. Divers were therefore instructed to wipe the instrument's optical window whenever in the field. Nevertheless, these measures were inadequate at times, resulting in an erroneously elevated fluorescence signal which had to be corrected. Erroneous fluorescence signals were identified in the time-series records by a sudden drop in the fluorescence signal when a diver manually wiped the instrument's optical window. For example, an elevated fluorescence signal resulting from biofouling occurred in September 2008 (Fig. 2A; note the sudden drop in the signal after cleaning (symbol D)). For this particular event, two different biofouling periods were identified. Because of the natural, diurnal fluctuation in the fluorescence signal, a line (identified as A–B in Fig. 2a) was drawn for the first period using the daily minimum values in the fluorescence data; this was accomplished using MATLAB data processing software (The MathWorks, Inc., Natick, MA, USA). The fluorescence values for this line were subtracted from the measured data over the first biofouling period. The second biofouling period, identified as B–C, was adjusted the same way, with the signal at C being lowered to the post-cleaning signal at D (Fig. 2A). The resulting corrected ECO FLNTU data are shown in Fig. 2B.

3.5. Depth integrations of upper-sediment porewater concentrations

Depth-integrated upper-sediment porewater inventories for dissolved inorganic nutrients and dissolved oxygen were calculated using the Curve Fitting Toolbox, a part of the MATLAB data processing software. All porewater concentrations were integrated to a depth of 10 cm below the SWI after applying a shape-preserving interpolant fit to the data. Standard deviations for the depth-integrated inventories were calculated using the standard deviations of the analytical replicates for each constituent, and then depth integrating the lower and higher analytical bounds. The median error for depth-integrated $Si(OH)_4$ and SRP were $\pm 1.3\%$ and $\pm 3.1\%$, respectively.

4. Results

4.1. Sediment and porewater characterization

The upper sediments (defined here to be the upper 10 cm) were determined to be >99% sand, with a phi value of 2.27 and phi standard deviation of 0.46, indicating a well sorted sediment (Folk and Ward, 1957). In contrast, the deeper sediment had greater heterogeneity, with large coral debris found at sediment depths of 15 cm and deeper. Sediment permeability, using the Carmen–Kozeny equation, and the sediment porosity at Kilo Nalu, were previously determined to be $\sim 8.8 \times 10$–$11\ m^2$ and 0.49, respectively (Hebert et al., 2007). The estimated sediment organic matter (or carbon) content of the upper sediments, determined by loss-on-ignition, was 4.64% ($SD = \pm 0.11$; data not shown). All DIC profiles peaked in the upper sediment (Fig. 3), with maximum values of 2.3–2.5 mM. XRD revealed that the upper sediment at Kilo Nalu is comprised of aragonite and magnesian calcite (data not shown).

Previous porewater sampling at Kilo Nalu conducted on two separate dates in 2006 indicated no salinity variation with sampling depth (Hebert et al., 2007). Samples collected and measured for chlorinity during the present study were consistent with the previous findings, with all porewater salinities being within 0.5% ($SD \pm 0.4$, $n = 22$) of the overlying water column salinity (data not shown).

4.2. July–August 2008: small surface gravity wave event

H_{sig} for this time period, during which four sets of porewater samples were collected, is plotted in Fig. 4. The mean H_{sig} for the week prior to the surface gravity event (indicated by a black line) was 0.71 m with a standard deviation of 0.10 m (indicated by the dashed lines), and is assumed to represent "background" conditions. The first two porewater samplings occurred during background conditions, with H_{sig} and V_{bed} averaging 0.71 m and 0.19 m/s, respectively. The third set of samples was collected at the peak of the swell. At this time, H_{sig} nearly doubled, reaching 1.30 m, and V_{bed} reached 0.35 m s^{-1}. The last porewater samples were collected after conditions had returned to background levels; H_{sig} and V_{bed} were 0.74 m and 0.19 m s^{-1}, respectively.

Samples collected during pre-swell background conditions showed enhanced SRP concentrations below the SWI, with a maximum of ~3 μM at a depth of 9.5 cm. Similarly, $Si(OH)_4$ concentrations were enhanced below the SWI, also reaching a maximum at 9.5 cm. At the peak of the swell event on 30 July, SRP and $Si(OH)_4$ concentrations in the 8-cm well were lowered to levels approaching that of the overlying water column. Maximum SRP concentrations were still observed at 9.5 cm, but maximum $Si(OH)_4$ concentrations were found deeper in the sediment (17.2 μM at 20.5 cm).

In the week prior to this swell event, mean turbidity and fluorescence remained mostly at background levels, using the background-period and graphical conventions defined for H_{sig} (see above; Fig. 4). The three-day running mean for turbidity more than doubled over

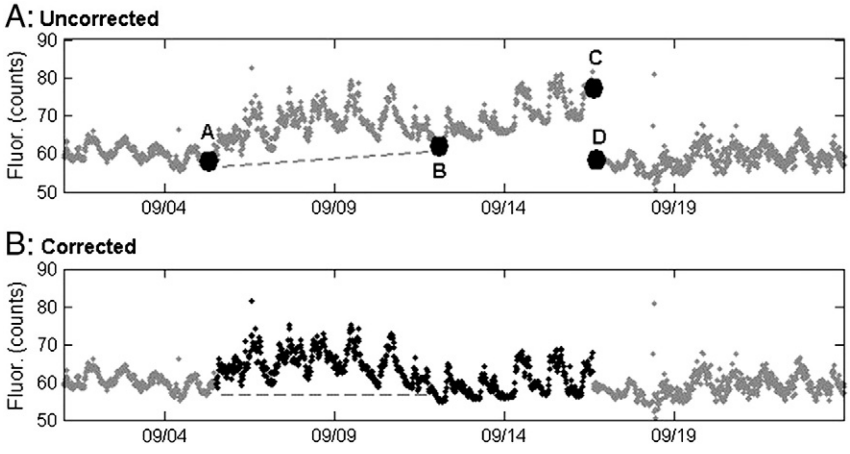

Fig. 2. Top panel: bottom-water fluorescence for 1–24 September 2008, before biofouling corrections. Bottom panel: bottom-water fluorescence for the same dates, after biofouling corrections; corrected data are shown in black. See text for details.

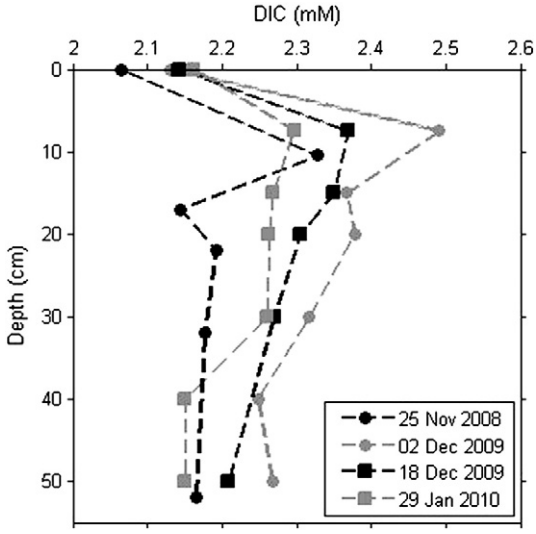

Fig. 3. Porewater and SWI DIC concentrations for 25 November 2008, 2 December 2009, 18 December 2009 and 29 January 2010. In this and subsequent figures, values plotted at zero depth represent samples collected just above the SWI (see text).

the background value during the peak of the swell event, while the fluorescence mean only increased slightly (data not shown). Following the swell, turbidity and fluorescence means returned to background conditions ~2 days after the swell peaked.

4.3. September 2008: larger surface gravity wave event

This larger swell event first reached Kilo Nalu on 4 September and resulted in H_{sig} increasing from background values of 0.60 m to a maximum of 1.6 m (Fig. 5). Similarly, V_{bed} averaged 0.18 m s^{-1} before the swell event and reached 0.49 m s^{-1} during the event. By the third sampling event, swell H_{sig} and V_{bed} had returned to background values.

Porewater samples were collected during background conditions, during the swell event, and after conditions had returned to background conditions. Although no sample was available, porewater DO concentrations before the swell event were assumed to be approximately zero at 8-cm depth, consistent with background samples collected at other times. On 9 September, during the swell, DO concentrations at 8-cm depth were ~200 μM, matching those of the overlying water column (Fig. 5). During the waning swell, on 16 September, DO concentrations at 8-cm depth decreased to 55 μM, before decreasing to background levels (near zero) on 24 September, after the swell. Similarly, both $Si(OH)_4$ and SRP in samples collected during background conditions, before and after the swell, showed enhancement over the overlying water column at the 8-cm depth, and reached maximum concentrations at 15 cm. Lower concentrations of $Si(OH)_4$ and SRP were observed at 8 cm during the swell and waning-swell sample days (Fig. 5).

For the week prior to the swell event, turbidity and fluorescence levels remained at background levels (Fig. 5). The swell resulted in a significant increase in both the turbidity and fluorescence records, and post-swell measurements showed a return to background conditions by the third discrete porewater sampling.

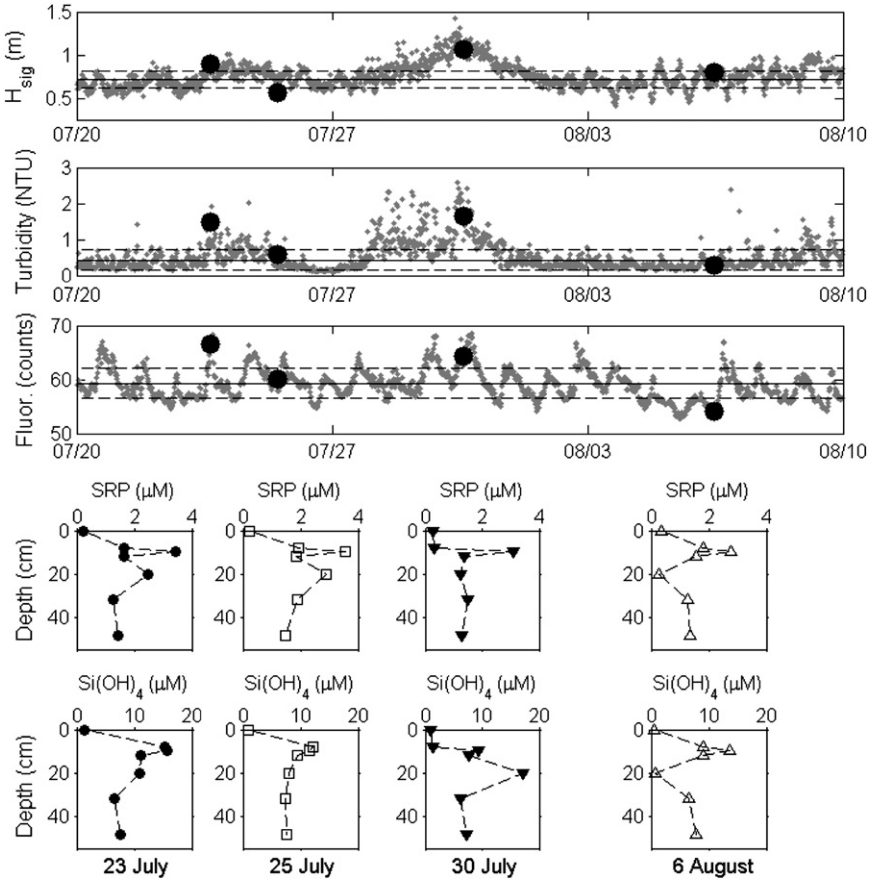

Fig. 4. Top panel: H_{sig} for 20 July–10 August 2008; each data point was calculated using 20 min of data. Second panel: mean bottom-water turbidity for the same time period. Third panel: mean bottom-water fluorescence for the same time period. Turbidity and fluorescence were measured ~0.5 m above the SWI; each data point represents a 20-min mean. Top three panels: Straight black line indicates mean levels for the week prior to swell event (background conditions); dashed lines represent the standard deviation of the mean for the same time period; black circles indicate porewater sampling dates. Bottom two panels: Porewater and SWI concentrations of SRP and $Si(OH)_4$ during 23 July–6 August 2008.

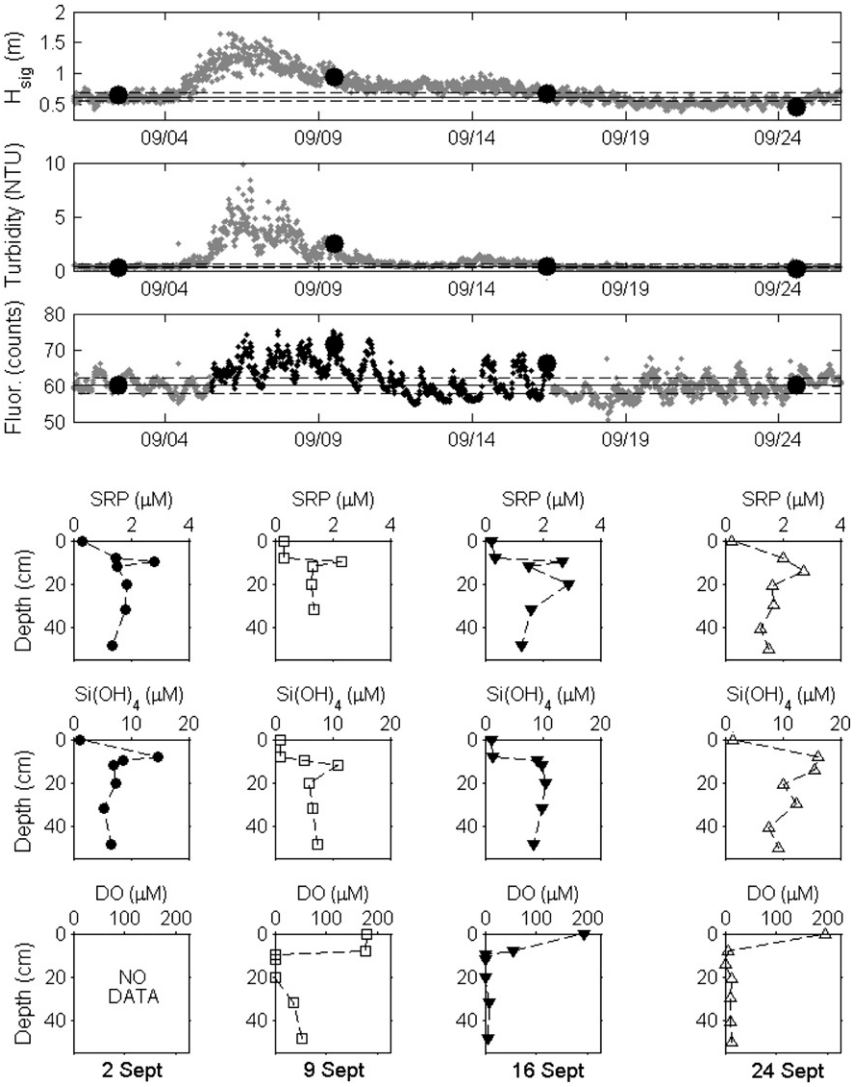

Fig. 5. Top panel: H_{sig} for 1–30 September 2008; each data point was calculated using 20 min of data. Second panel: mean bottom-water turbidity for the same time period. Third panel: mean bottom-water fluorescence for the same time period. Turbidity and fluorescence were measured ~0.5 m above the SWI; each point represents a 20-min mean. Black data points indicate that data were corrected for biofouling (See Methods). Top three panels: Straight black lines indicate mean levels for the week prior to swell event (background conditions); dashed lines represent the standard deviation of the mean for the same time period; black circles indicate porewater sampling dates. Bottom three panels: Porewater and SWI concentrations for SRP, $Si(OH)_4$ and DO during 2–24 September 2008. The 2 September SWI values represent mean concentrations from 25 other sampling dates.

4.4. December 2008: Large Kona swell event

Porewater sampling in December 2008 were carried out during a Kona swell that had large peaks in both wave height (Fig. 6) and freshwater input (Fig. 7). Note that there was no appreciable freshwater input to the system during the first two swell events. H_{sig} reached a maximum of 2.9 m on 11 December, significantly above background conditions observed during the prior week. Similarly, V_{bed} also peaked on 11 December at 0.64 m s^{-1}, four times the background value. A second peak in the storm's intensity resulted in a maximum H_{sig} of 2.4 m and a maximum V_{bed} of 0.48 m s^{-1} on 13 December. The two pulses of the storm are also evident in the surface turbidity record, with maxima at WQB-AW and WQB-KN buoys (Fig. 1) of 14.0 and 6.6 NTU, respectively (data not shown). Background conditions had returned by the second porewater sampling on 15 December (Fig. 6).

Before the swell event, background porewater SRP concentrations reached a maximum of 2.14 μM at 10.5 cm below the SWI, while $Si(OH)_4$ reached a maximum of 21.5 μM. When background conditions had returned after the swell, SRP was reduced by ca. half, while $Si(OH)_4$ was reduced by ~85% (Fig. 6).

Each increase in swell was accompanied by an increase in freshwater input. Rain gauges located at ALO and MLA (Fig. 1) recorded 10.0 and 18.6 cm of rainfall, respectively, over ~18 h on 11 December (Fig. 7). By 14 December, 13.2 and 27.5 cm of rain had fallen at ALO and MLA, respectively, during this three-day storm. Prior to the storm, flow in the Mānoa–Pālolo Drainage Canal was below estimated mean base flow, but, as the storm peaked on 11 December, the highest flow of 2008 was reached, with 72 m^3 s^{-1} recorded at the USGS 26247100 stream gauge (Fig. 1), ~450 times mean base flow (Tomlinson et al., 2011). Freshwater input, measured at the WQB-AW and WQB-KN buoys at ~1 m below the surface, resulted in lowered ocean surface salinities, from ~35 to 30.5 and 32.4, respectively (data not shown). The freshwater signal was also observed in the bottom water at Kilo Nalu, with a drop in the salinity from 35.1 to 34.6, the largest salinity change seen in the previous 6 months at Kilo Nalu (Fig. 7).

There was a significant increase in the turbidity and fluorescence levels in the bottom water during the storm (Fig. 6). At the storm's peak on 11 December, turbidity levels were sustained above 20 NTU for several hours. As background swell conditions returned on 15 December, nearly background turbidity levels returned to the bottom

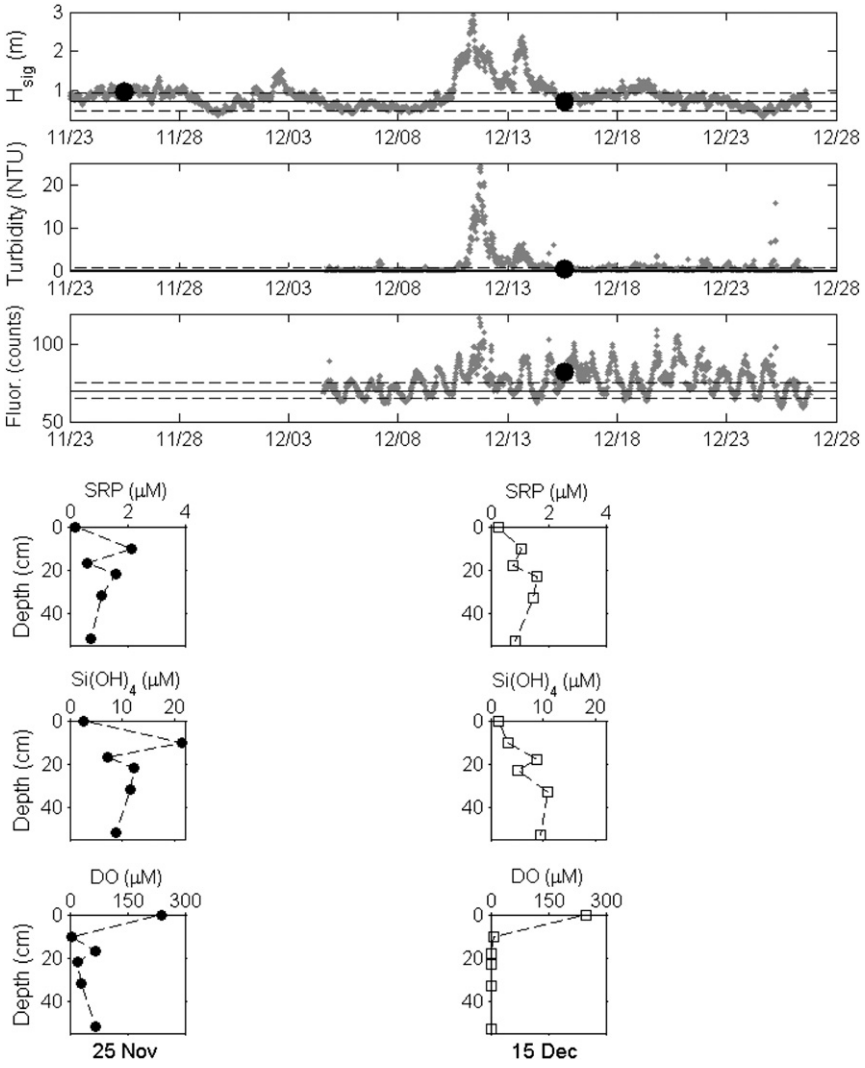

Fig. 6. Top panel: H_{sig} for 23 November–28 December 2008; each data point was calculated using 20 min of data. Straight black line indicates mean levels for the week prior to swell event (background conditions); dashed lines represent the standard deviation of the mean for the same time period; black circles indicate porewater sampling dates. Second panel: mean bottom-water turbidity for the same time period. Third panel: mean bottom-water fluorescence for the same time period. Turbidity and fluorescence were measured ~0.5 m above the SWI; each data point representing a 20-min mean. Second and third panels: Straight black lines indicate mean levels for 4 days prior to swell event (background conditions); dashed lines represent the standard deviation of the mean for the same time period; black circles indicate porewater sampling dates. Bottom three panels: Porewater and SWI concentrations of SRP, $Si(OH)_4$ and DO at Kilo Nalu on 25 November and 15 December 2008.

water, while the elevated fluorescence signal was sustained for about a week post-swell.

5. Discussion

5.1. Porewater flushing and biological response to swell events

Surface gravity waves have been shown to be important in enhancing fluid exchange in permeable sediments (see Introduction), and this effect was observed in both the July and September events in our study. The flushing of the upper sediment during these events resulted in $Si(OH)_4$ and SRP porewater concentrations matching those of the overlying water column (Figs. 4 and 5), and the full oxygenation of the upper sediment during the September swell event (Fig. 5). Subsequent depletion of DO in the upper sediment was captured in porewater sampling during the waning of the September swell, with DO levels decreasing to 55 μM in the upper sediment by 16 September (Fig. 5). During the December Kona swell event, the less depleted dissolved nutrient concentrations and less enhanced DO concentrations in the sediment (Fig. 6; compared to the other swell events) are likely a consequence of porewater sampling during post-swell conditions (as opposed to during the swell peak) and reflect changes in sediment metabolism due to organic matter injection, as discussed below.

Each swell event showed a significant increase in bottom water turbidity during the swell, followed by a return to background levels post-swell (Figs. 4–6). This increased turbidity was measured ~0.5 m above the SWI, suggesting that there was significant disturbance and resuspension of the sediment at the SWI. The corresponding increases in fluorescence (Figs. 4 and 5) during the first two swell events (July and September 2008) indicates that there was either an increase in biological productivity or a suspension of benthic phototrophs into the water column during the events, with available data unable to distinguish between the two. The fact that increased fluorescence levels were not sustained during the first two swells, and quickly returned to ca. background levels post-swell, suggest that the suspended phototrophs had settled out, or had penetrated the SWI and were trapped in the sediment. In contrast, the fluorescence level increase observed during the third and largest swell was maintained post-swell (Fig. 6), suggesting a persistent photosynthetic response.

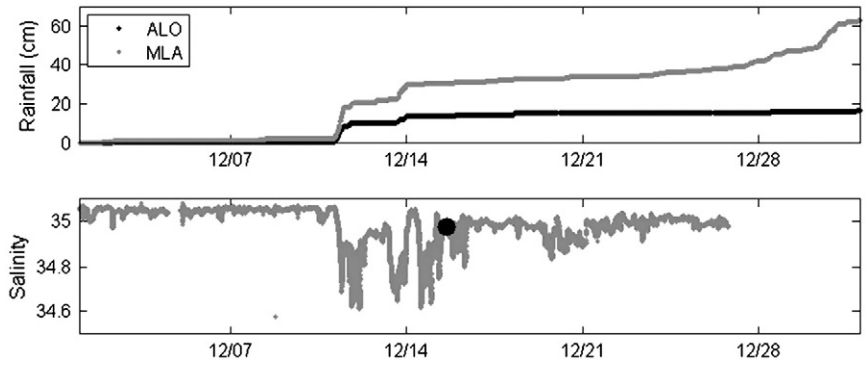

Fig. 7. Top panel: cumulative rainfall from rain gauges, starting 1 December 2008; Mānoa Lyon Arboretum (MLA) data are shown in gray and Aloha Tower (ALO) data are shown in black. Bottom panel: bottom-water salinity ~0.5 m above the SWI; black circle indicates porewater sampling date.

5.2. Dissolved oxygen and nutrient inventories

Upper-sediment inventories were calculated for the 18 porewater samplings during the intensive sampling period from June to December 2008, including those during the three swell events described previously. Porewater nutrient and DO profiles were numerically integrated to 10 cm depth, the depth to which porewater flushing was observed (See Depth-Integrations of Porewater Concentrations). Integrations were then corrected for a sediment porosity of 0.49. Bottom-water inventories were calculated using the SWI concentrations, which were arbitrarily assumed to be constant throughout the bottom 1 m of the water column.

5.2.1. Sediment dissolved oxygen inventories

Porewater composition results in part from sediment metabolism, reflecting a balance between organic matter reactivity and viable electron acceptor availability (e.g., Falter and Sansone, 2000a; Froelich et al., 1979). Surface gravity waves can control the availability of electron acceptors in permeable sediments by flushing the sediment with DO and other oxidants. Thus, porewater composition in such environments should vary with changes in wave height (Falter and Sansone, 2000a). This relationship is evident when examining the upper-sediment DO inventory versus mean V_{bed} for June to December 2008 (Fig. 8). Mean V_{bed} for this plot is computed for the six hours previous to porewater collection. The linear DO-V_{bed} relationship suggests that an increase in V_{bed} (associated with increasing H_{sig}) increases the rate of DO replenishment to the system (Falter and Sansone, 2000a), resulting in an increased oxygenation of the sediments with increasing H_{sig} and V_{bed}.

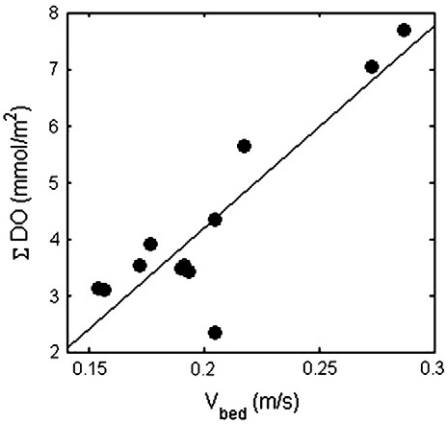

Fig. 8. Upper-sediment (0–10 cm) DO inventory versus mean V_{bed} ($y = 36x - 2.9$, $R^2 = 0.79$). Mean V_{bed} was calculated using velocities from the 6 h prior to porewater sampling. Data collected during June–December 2008.

If an increase in swell size was the only variable affecting DO inventories, then one would expect the largest swells to result in the greatest total-sediment DO inventories, but this was not the case. During the largest of the swells, the Kona storm in December 2008, DO was depleted ~10 cm below the SWI (Fig. 6). This event was unique because we observed not only large swell heights and nearbed velocities, but also a large amount of freshwater runoff (with associated organic matter) entering the system (Fig. 7; Tomlinson et al., 2011). Thus, the increased delivery of terrestrial particulate organic matter during this swell event may have caused an increase in sediment metabolism, as seen previously in other coastal Hawaiian waters (De Carlo et al., 2007). This increase in sediment metabolism may exceed the rate of DO replenishment, leading to short-term upper-sediment DO depletion, as seen elsewhere on O'ahu (Falter and Sansone, 2000a).

5.2.2. Nutrient inventories

Upper-sediment inventories (0–10 cm) were calculated for SRP and $Si(OH)_4$. By removing the four sample dates for which the upper sediment were affected by swell events (30 July 2008, 9 and 16 September 2008, and 15 December 2008), the remaining upper-sediment inventories represent a potential nutrient source that could be added to the bottom water in a complete flushing of the upper sediment during a swell event. The mean upper-sediment SRP inventory was 61 ($\pm$12) μmol m^{-2}, while the mean bottom-water SRP inventory was 270 ($\pm$42) μmol m^{-2}. If flushed out in a single pulse by a swell event, the upper-sediment inventory would increase the bottom-water SRP inventory an average of ~23% ($\pm$5.7%).

The mean bottom-water inventory of $Si(OH)_4$ at Kilo Nalu was 1300 μmol m^{-2}, with a large standard deviation of $\pm$680, resulting from SWI concentrations being at or just above the limit of detection for the analytical method. Mean upper-sediment $Si(OH)_4$ inventories were 620 ($\pm$220) μmol m^{-2}. Consequently, the potential increase in the bottom-water $Si(OH)_4$ inventory due to the flushing of the upper-sediment $Si(OH)_4$ inventory varied widely, with a mean of ~65% ($\pm$30%), making this calculation less robust.

Although this calculation estimates a possible SRP enhancement of almost 25% in the bottom water during swell events, the effect this enhancement could have on phytoplankton populations at Kilo Nalu cannot presently be determined. Furthermore, the application of this calculation is weakened by only considering a single flushing of the upper sediment, ignoring the rate at which sediment metabolism normally replenishes the nutrient inventories (discussed below). Lastly, the freshwater runoff that perturbed most of the water column during the December storm event (Fig. 7) contained nutrients and organic matter that may have contributed to the enhanced fluorescence response in the bottom water (Tomlinson et al., 2011). De Carlo et al. (2007) hypothesized that sustained water-column productivity observed long after strong storm runoff along O'ahu reflects benthic release of nutrients from remineralization of allochthonous organic

matter delivered during storms. The delivery of additional nutrients and organic material may have been a reason why a sustained fluorescence response was observed during the December 2008 swell and not during the previous two.

5.3. Constraints on nutrient transport

The porewater transport/exchange rate and the organic matter remineralization rate must both be considered when determining the controls on nutrient supply to (and the DO removal from) the overlying water. The transport rates in the sediments at Kilo Nalu have been numerically modeled by Jon Fram (personal communication, 2012) using verification data from field experiments performed at Kilo Nalu. Given a wave height of 0.65 m and a period of 13 s, and the water-column depth at Kilo Nalu (12 m), the upper sediment (~10 cm) is flushed by the overlying seawater in under 6 h. While remineralization rates are difficult to measure in situ, Sansone et al. (1990) demonstrated the existence of high rates of aerobic respiration in batch incubations of Hawaiian carbonate sands similar to the ones found at Kilo Nalu: they found that no porewater DO remained 5 h after the start of the incubations. Thus, the rates of transport and remineralization are likely to be similar in our sediment. The following section uses our porewater DO and nutrient time-series data to provide additional information on the rate of sediment remineralization.

5.4. Upper-sediment recovery

A plot of upper-sediment DO inventories for the September swell event vs. time was used to represent the upper-sediment aerobic respiration following complete oxygenation of the upper sediment during the swell event (Fig. 9): DO is consumed linearly vs. time in these sediments, with the porewater reaching background (non-swell) DO levels in 15 days. This corresponds to an apparent upper-sediment de-oxygenation rate of 0.31 mmol m^{-2} d^{-1}. The longer DO depletion times observed at Kilo Nalu, compared to the non-aerated batch incubations of Sansone et al. (1990), was likely due to advective transport of oxygenated bottom water into the Kilo Nalu sediment. Note that no DO measurements were carried out during the July swell, and the December swell event was not included in this analysis because no sampling occurred post-swell.

Upper-sediment nutrient inventories (0–10 cm) for the July and September swell events were similarly plotted against time to examine the recovery of porewater nutrient inventories following complete flushing during swell events (Fig. 10). For both $Si(OH)_4$ and SRP, upper-sediment inventories were seen to increase linearly with time, even when combining data from the two separate swell events. The recovery of upper-sediment nutrient inventories depends on both porewater transport and remineralization rates. Mean V_{bed} was 0.19 (±0.022) and 0.17 (±0.028) m s^{-1}, respectively, when sampling occurred after the July and September swells; thus, SWI transport rates can be assumed to be relatively constant. Note that the deviation from the regression in the $Si(OH)_4$ plot (Fig. 10) occurred primarily during the second, smaller peak of the September event when physical conditions were still elevated over background values. The linear relationship of upper-sediment nutrient inventories over time and the near-constant transport rates suggest that remineralization rates must have been generally constant in the upper sediment. Although in-situ remineralization rates cannot presently be quantified since part of the nutrient inventory has been lost in transport to the overlying bottom water, upper-sediment recovery rates for Si(OH)4 and SRP were 35 μmol m^{-2} d^{-1} and 3.5 μmol m^{-2} d^{-1}, respectively.

Jahnke et al. (2005) also observed relatively constant remineralization rates in permeable South Atlantic Bight (SAB) sediments during incubation experiments done with constant mixing of the overlying water. Whereas $Si(OH)_4$ remineralization rates for the SAB were calculated to be larger than the sediment inventory recovery rates found at Kilo Nalu, sediment in the SAB was 3 order of magnitude less permeable than those found at Kilo Nalo. Also, it is not clear how comparable our in-situ results are to the incubated cores of Jahnke et al. (2005), given the complications involved in the laboratory incubations of hydrodynamically active permeable sediments. Regardless, we choose to label our measurements of the rate of change of porewater inventories simply as "inventory recovery rates" (rather than "estimated remineralization rates", as done by Jahnke et al. (2005)) because the concentration changes are dependent on both the remineralization rate and the porewater–seawater exchange rate.

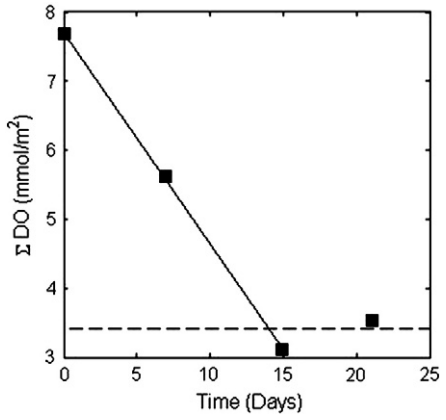

Fig. 9. Upper-sediment (0–10 cm) DO inventory versus time for September 2008 swell event ($y=-0.31x+7$, $R^2=1$). Time is defined as the days since the porewater sampling first demonstrated flushing of the upper sediment during the swell event. Dashed line represents the background (non-swell) upper-sediment DO inventory of 3.4 (± 0.56) mmol/m^2,which is the mean of DO inventories measured during background conditions throughout the intensive sampling period of June to December 2008.

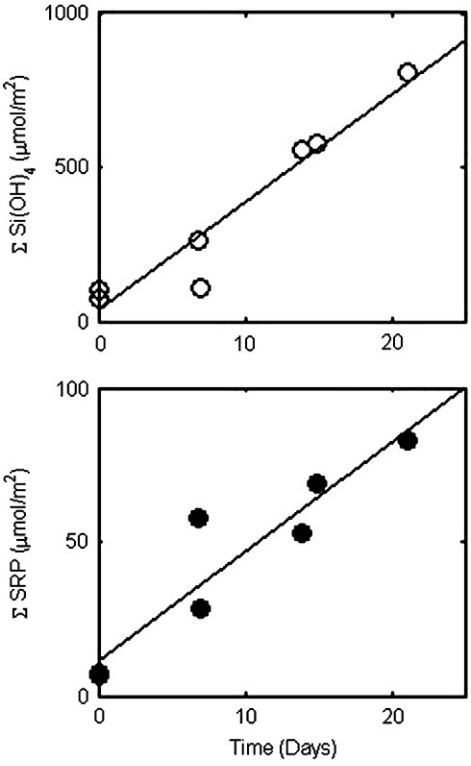

Fig. 10. Top panel: Upper-sediment (0–10 cm) $Si(OH)_4$ inventory versus time for July and September 2008 swell events. ($y=35x+34$, $R^2=0.93$). Bottom panel: Upper-sediment SRP inventory versus time for July and September 2008 swell events ($y=3.5x+11$, $R^2=0.88$). Time is defined as the days since the porewater sampling first demonstrated flushing of the upper sediment during a swell event.

During the September swell event, DO upper-sediment inventories were observed to return to mean inventories within 15 d of porewater flushing. Nevertheless, during this same swell event, both the $Si(OH)_4$ and SRP upper-sediment inventories were seen to increase linearly through 21 d, suggesting that remineralization continues at a relatively constant rate in the upper sediment even after the sediment becomes suboxic. This is consistent with studies conducted at Checker Reef, Hawaii (Falter and Sansone, 2000a; Tribble et al., 1990) that established the importance of suboxic processing in similar sediments.

5.5. DIC-nutrient relationships

As organic matter undergoes remineralization, DIC and inorganic nutrients are produced (e.g., Froelich et al., 1979). During background conditions at Kilo Nalu, porewater DIC, SRP and $Si(OH)_4$ concentrations exceed those at the SWI, and remineralized SRP and $Si(OH)_4$ were linearly correlated with remineralized DIC (Fig. 11). Remineralized concentrations are defined here as the increase in porewater concentration above SWI concentrations ($X_{REMIN} = X_{PW} - X_{SWI}$), with the increase presumably reflecting the effects of remineralization. Using the slopes from these plots, we recorded a molar inorganic carbon-to-phosphorus (C:P) ratio of 170 ($R^2 = 0.31$) and a molar inorganic carbon-to-silicate (C:Si) ratio of 27.8 ($R^2 = 0.74$) in the porewater.

Inorganic C:P ratios can be used to characterize the organic source matter undergoing remineralization in the sediment (Ibarra-Obando et al., 2004). We assume that the majority of the organic matter deposited onto the Kilo Nalu sediment is marine in origin, except in the case of intense localized storms (discussed above). We also use the C: P ratio for coastal plankton off of Honolulu (~81:1; Laws et al., 1984), and the global median organic C: P ratio for benthic macroalgae and seagrasses (550:1; Atkinson and Smith, 1983) to define the marine organic end-members. Using these ratios and a two-end-member mixing model with planktonic and benthic end-members, and assuming an average C:P ratio for Kilo Nalu remineralization of 170 (Fig. 10), the source organic matter to the sediments at Kilo Nalu is estimated to be 81% planktonic and 19% benthic. This estimate assumes complete remineralization of organic matter and assumes that the metabolic CO_2 (DIC) generated by oxic degradation of organic matter does not lead to $CaCO_3$ dissolution and additional DIC (see discussion below). Also, it ignores possible abiotic processes (adsorption to carbonate particles) that can affect remineralized phosphate levels (e.g., Fox et al., 1986; Froelich, 1988), which could be why the C:P correlation is weak ($R^2 = 0.31$).

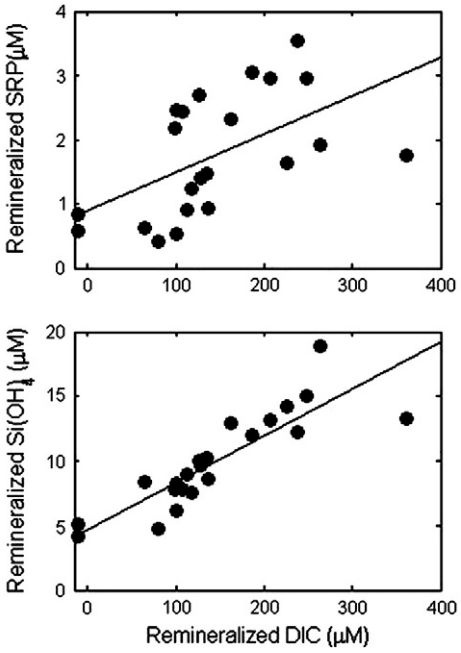

Fig. 11. Top panel: remineralized SRP versus remineralized DIC ($y = 0.0059x + 0.91$, $R^2 = 0.31$). Bottom panel: remineralized $Si(OH)_4$ versus remineralized DIC ($y = 0.036x + 4.7$, $R^2 = 0.74$). Remineralized values are porewater concentrations minus corresponding SWI concentration ($X_{REMIN} = X_{PW} - X_{SWI}$). Data are from background conditions.

Although taxonomic information is currently unavailable for plankton being deposited in Kilo Nalu sediment, both planktonic and/or benthic diatoms have been seen to be important sources of organic matter to coastal permeable sediments (Jahnke et al., 2005). The strong DIC:Si relationship (Fig. 10) indicates a good correlation between Si released to porewater and organic matter remineralization, as commonly seen in similar sediments (e.g., Tribble et al., 1990). Deviation from the DIC:Si correlation could result if excess Si was abiotically added to the porewater. In Hawai'i, processes such as submarine groundwater discharge to the sediment could be responsible for excess Si, but the strong DIC:Si correlation and porewater chlorinity data (see Results) suggest that submarine groundwater discharge on the system is null or negligible. Hence, planktonic and/or benthic diatoms may be important sources of organic matter to the sediment at Kilo Nalu, as seen in other permeable sediments (e.g., Jahnke et al., 2005).

Deviation from the DIC:Si correlation would also result if abiotic processes were adding or removing carbon, such as calcium carbonate dissolution or precipitation, respectively. While both of these processes are known to occur in carbonate sediments, no strong evidence for either process occurring in the sediment at Kilo Nalu currently exists. The strong DIC:Si relationship (discussed above) indicates that the majority of DIC results from organic matter remineralization. Additionally, no significant build-up or removal of Ca^{2+} was seen on three porewater sampling dates (data not shown).

6. Conclusions

Swell events were observed to enhance fluid exchange between the upper sediment and the overlying water column at Kilo Nalu, resulting in short time-scale variability in the porewater concentrations of DO and inorganic nutrients. This short-term variability was associated with changes in surface gravity wave heights and nearbed currents. This variability in the physical environment was also linked to particulate loads and fluorescence levels in the bottom water at Kilo Nalu.

The nearbed current velocity was correlated with upper-sediment DO inventories, suggesting that increasing oxygenation of the sediment occurs with larger H_{sig} and V_{bed}. Nutrient and DO upper-sediment inventories were seen to recover linearly after swell events; DO inventories recovered faster than nutrient inventories, indicating that suboxic diagenesis occurs in the upper sediment. Ratios of regenerated nutrients indicate that the majority of the organic matter undergoing remineralization in the Kilo Nalu sediment is planktonic in origin.

Although challenging, direct measurements of SWI fluxes and sediment remineralization rates would help constrain estimates of transport rates. Additionally, investigation into the dominant processes affecting these environments, including the role of benthic remineralization, organic matter loading, and physical drivers, would help improve scientific understanding of these complex environments and their potentially important, and largely underestimated, role in global biogeochemical cycles.

Acknowledgments

We thank Chris Colgrove and Jon Fram for their logistical assistance and support throughout this study; Judith Wells, Brian McLaughlin, and Jeff Sevadjian for help in data processing and instrument management; Keo Lopes and Kimball Millikan for assistance in the field;

Margaret McManus for her input and guidance throughout the research and writing process; and Geno Pawlak for the generous use of the Kilo Nalu Observatory and its infrastructure during the course of this study. This research was supported by US National Science Foundation grants OCE-0536607 and OCE-1031947. U.H. School of Earth and Science Technology contribution no. 8810.

References

Atkinson, M.J., Smith, S.V., 1983. C:N:P ratios of benthic marine plants. Limnol. Oceanogr. 28 (3), 568–574.
Boudreau, B.P., Huettel, M., Forster, S., Jahnke, R.A., McLachlan, A., Middelburg, J.J., Nielson, P., Sansone, F.J., Taghon, G., Van Raaphorst, W., Webster, I., Weslawski, J.M., Wiberg, P., Sundby, B., 2001. Permeable marine sediments: overturning an old paradigm. Eos, Trans. Amer. Geophys. Union 82 (11), 133–136.
De Carlo, E.H., Hoover, D.J., Young, C.W., Hoover, R.S., Mackenzie, F.T., 2007. Impact of storm runoff from subtropical watersheds on coastal water quality and productivity. Appl. Geochem. 22 (8), 1777–1797.
Dean, W.E., 1974. Determination of carbonate and organic matter in calcareous sediments and sedimentary rocks by loss on ignition: comparison with other methods. J. Sediment. Petrol. 44 (1), 242–248.
Dickson, A.G., Sabine, C.L., Christian, J.R. (Eds.), 2007. Guide to Best Practice for Ocean CO_2 Measurements. PICES Special Publication, 3. North Pacific Marine Science Organization, Sidney, British Columbia (191 pp.).
Emery, Thomson, 2004. Data Analysis Methods in Physical Oceanography. Elsevier, San Diego (638 pp.).
Falter, J.L., Sansone, F.J., 2000a. Hydraulic control of pore water geochemistry within the oxic-suboxic zone of a permeable sediment. Limnol. Oceanogr. 45 (3), 550–557.
Falter, J.L., Sansone, F.J., 2000b. Shallow pore water sampling in reef sediments. Coral Reefs 19 (1), 93–97.
Fletcher, C.H., Grossman, E.E., Richmond, B.M., Gibbs, A.E., 2002. Atlas of Natural Hazards in the Hawaii Coastal Zone. U.S. Geological Survey, Denver (182 pp.).
Fogaren, K.E., 2010. Short-time Scale and Seasonal Variability of Porewater Constituents in a Permeable Nearshore Sediment. M.S. Thesis, University of Hawaii at Manoa, Honolulu, 86 pp.
Folk, R.L., Ward, W.C., 1957. Brazos River Bar: a study in the significance of grain size parameters. J. Sediment. Petrol. 27 (1), 3–26.
Fox, L.E., Sager, S.L., Wofsy, S.C., 1986. The chemical control of soluble phosphorus in the Amazon estuary. Geochim. Cosmochim. Acta 50 (5), 783–794.
Froelich, P.N., 1988. Kinetic control of dissolved phosphate in natural rivers and estuaries: a primer on the phosphate butter mechanism. Limnol. Oceanogr. 33 (4), 649–668.
Froelich, P.N., Klinkhammer, G.P., Bender, M.L., Luedtke, N.A., Heath, G.R., Cullen, D., Dauphin, P., 1979. Early oxidation of organic matter in pelagic sediments of the eastern equatorial Atlantic: suboxic diagenesis. Geochim. Cosmochim. Acta 43 (7), 1075–1090.
Fryer, P., 1995. The 1991–1992 NSF Young Scholars Program and the University of Hawaii: Science and Engineering Studies of the Ala Wai Canal, an Urban Estuary in Honolulu. Pac. Sci. 49 (4), 319–331.
Grasshoff, K., Ehrhardt, M., Kremling, K., 1983. Methods of Seawater Analysis. Wiley-VCH, Weinheim (419 pp.).
Grigg, R.W., 1995. Coral reefs in an urban embayment in Hawaii: a complex case history controlled by natural and anthropogenic stress. Coral Reefs 14 (4), 253–266.
Hebert, A.B., Sansone, F.J., Pawlak, G.R., 2007. Tracer dispersal in sandy sediment porewater under enhanced physical forcing. Cont. Shelf Res. 27 (17), 2278–2287.
Heiri, O., Lotter, A.F., Lemcke, G., 2001. Loss on ignition as a method for estimating organic and carbonate content in sediments: reproducibility and comparability of results. J. Paleolimnol. 25, 101–110.
Huettel, M., Gust, G., 1992. Impact of bioroughness on interfacial solute exchange in permeable sediments. Mar. Ecol. Prog. Ser. 89, 253–267.
Huettel, M., Rusch, A., 2000. Transport and degradation of phytoplankton in permeable sediment. Limnol. Oceanogr. 45 (3), 534–549.
Huettel, M., Ziebis, W., Forster, S., 1996. Flow-induced uptake of particulate matter in permeable sediments. Limnol. Oceanogr. 41 (2), 309–322.
Huettel, M., Ziebis, W., Forester, S., Luther III, G.W., 1998. Advective transport affecting metal and nutrient distributions and interfacial fluxes in permeable sediments. Geochim. Cosmochim. Acta 62 (4), 613–631.
Ibarra-Obando, S.E., Smith, S.V., Poumian-Tapia, M., Camacho-Ibar, V., Carriquiry, J.D., Montes-Hugo, M., 2004. Benthic metabolism in San Quintin Bay, Baja California, Mexico. Mar. Ecol. Prog. Ser. 283, 99–112.
Jahnke, R.A., 2004. Transport processes and organic matter in coastal sediments. In: Robinson, A.R., Brink, K. (Eds.), The Sea, Volume 13: The Global Coastal Ocean. Harvard University Press, Harvard, pp. 163–192.
Jahnke, R.A., Nelson, J., Marinelli, R.L., Eckman, J.E., 2000. Benthic flux of biogenic elements on the Southeastern US continental shelf: influence of pore water advective transport and benthic microalgae. Cont. Shelf Res. 20 (1), 109–127.
Jahnke, R.A., Richards, M., Nelson, J., Robertson, C., Rao, A., Jahnke, D., 2005. Organic matter remineralization and porewater exchange rates in permeable South Atlantic Bight continental shelf sediments. Cont. Shelf Res. 25 (12–13), 1433–1453.
Laws, E.A., Redalje, D.G., Haas, L.W., Bienfang, P.K., Eppley, R.W., Harrison, W.G., Karl, D.M., Marra, J., 1984. High phytoplankton growth and production rates in oligotrophic Hawaiian coastal waters. Limnol. Oceanogr. 29 (6), 1161–1169.
Laws, E.A., Ziemann, D., Schulman, D., 1999. Coastal water quality in Hawaii: the importance of buffer zones and dilution. Mar. Environ. Res. 48 (1), 1–21.
Meyer-Reil, L.A., 1986. Spatial and temporal distribution of bacterial populations in marine shallow water surface sediments. In: Lasserre, P., Martin, J.M. (Eds.), Biogeochemical Processes at the Land-Sea Boundary. Elsevier/North-Holland Publishing Co., Amsterdam, pp. 141–160.
Moberly, R.J., Chamberlain, T., 1964. Hawaiian beach systems. Technical Report 64–2. Hawaii Institute of Geophysics, University of Hawaii, Honolulu.
Riedl, R.J., Huang, N., Maohan, R., 1972. The subtidal pump: a mechanism of interstitial water exchange by wave action. Mar. Biol. 13 (3), 210–221.
Rocha, C., 2008. Sandy sediments as active biogeochemical reactors: compound cycling in the fast lane. Aquat. Microb. Ecol. 53 (1), 119–127.
Rusch, Huettel, M., 2000. Advective particle transport into permeable sediments–evidence from experiments in an intertidal sandflat. Limnol. Oceanogr. 45 (3), 523–533.
Sansone, F.J., Tribble, G.W., Andrews, C.C., Chanton, J.P., 1990. Anaerobic diagenesis within Recent, Pleistocene, and Eocene marine carbonate frameworks. Sedimentology 37, 997–1009.
Sansone, F.J., Pawlak, G., Stanton, T.P., McManus, M.A., Glazer, B.T., Decarlo, E.H., Bandet, M., Sevadjian, J., Stierhoff, K., Colgrove, C., Hebert, A.B., Chen, I.C., 2008. Kilo Nalu physical/biogeochemical dynamics above and within permeable sediments. Oceanography 21 (4), 173–178.
Skoog, D.A., West, D.M., Holler, F.J., 1994. Analytical Chemistry: An Introduction. Saunders College Publishing, Philadelphia (612 pp.).
Tomlinson, M.S., De Carlo, E.H., McManus, M.A., Pawlak, G., Steward, G.F., Sansone, F.J., Nigro, O.D., Timmerman, R.E., Patterson, J., Jaramillo, S., Ostrander, C.E., 2011. Characterizing the effects of two storms on the coastal waters of O'ahu, Hawai'i, using data from the Pacific Islands Ocean Observing System. Oceanography 24 (2), 182–199.
Tribble, G.W., Sansone, F.J., Smith, S.V., 1990. Stoichiometric modeling of carbon diagenesis within a coral reef framework. Geochim. Cosmochim. Acta 54, 2439–2449.
Webb, J.E., Theodor, J., 1968. Irrigation of submerged marine sands through wave action. Nature 220, 682–683.